Accurate calibration method for a structured light system

Zhongwei Li
Yusheng Shi
Congjun Wang
Yuanyuan Wang
Huazhong University of Science and Technology
State Key Laboratory of Material Processing
and Die & Mould Technology
Wuhan, 430074, China

Abstract. System calibration is crucial for any 3-D shape measurement system. An accurate method is proposed to calibrate a 3-D shape measurement system based on a structured light technique. The projector is treated as a camera to unify the calibration procedures of a structured light system and a well-established stereo vision system. The key to realizing this method is to establish a highly accurate correspondence between camera pixels and projector pixels and generate digital micromirror device (DMD) image sets for projector calibration. A phase-shifting method is used to accomplish this task. A precalibrated lookup table and a linear interpolation algorithm are proposed to improve the accuracy of the generated DMD image, and accordingly improve the accuracy of the projector calibration and the 3-D measurement. Some experimental results are presented to demonstrate the performance of the system calibration.
[DOI: 10.1117/1.2931517]

Subject terms: structured light system; system calibration; projector calibration; phase-shifting method; error compensation.

Paper 071018RR received Dec. 27, 2007; revised manuscript received Feb. 27, 2008; accepted for publication Mar. 4, 2008; published online May 29, 2008.

1 Introduction

The automatic, noncontact measurement of objects in industrial applications is one of the most important applications of 3-D shape measurement methods.[1,2] Among the existing 3-D shape measurement techniques, structured-light-based techniques are increasingly used, due to their high speed and noncontact nature. A structured light system differs from a classic stereo vision system in that it avoids the fundamentally difficult problem of stereo matching by replacing one camera with a light-pattern projector. The key to accurate reconstruction of the 3-D shape is the proper calibration of each element used in the structured light system.[3]

Several approaches to calibrating structured light systems can be found in the literature, such as techniques based on neural networks,[4,5] bundle adjustment,[6–11] or absolute phase,[12] in which the calibration process depends on the available system parameter information and the system setup. They usually involve complicated and time-consuming procedures. A novel method of treating the projector as a camera was proposed to unify the calibration procedures of a structured light system and a classic stereo vision system.[3,13] This method uses a camera to capture images "for" the projector and then transforms the images into projector images, so that they are as if captured directly by the projection chip [digital micromirror device (DMD)] in the projector. The key to realizing this method is to establish the correspondence between camera pixels and projector pixels. The accuracy of the correspondence is one of the key factors that influence the calibration accuracy. References 3 and 13 use a phase-shifting method is used to accomplish this task. This method is simple and fast, but they do not address the effect of the nonlinear γ of the projector,[14] which introduces phase error and affects the accuracy of the correspondence.

In this work, we also use a phase-shifting method to establish the correspondence between camera pixels and projector pixels. Furthermore, we propose two procedures to improve the accuracy of the projector calibration. We analyzed the effect of the nonlinear γ of the projector and built a lookup table (LUT) to reduce the error of the actual phase value. This process can get a more accurate unwrapped absolute phase map, which can improve the accuracy of the correspondence between camera pixels and projector pixels. Because the data set used for camera calibration was of subpixel precision, a linear interpolation method was utilized to calculate the corresponding DMD image coordinates. This method can achieve DMD images with subpixel precision. These two processes can greatly improve the accuracy of the correspondence of the DMD image and accordingly improve the accuracy of the projector calibration and the 3-D measurement.

The organization of the work is as follows: In Sec. 2, a description of the calibration procedure is given. In Sec. 3, some experiments are reported that evaluate the calibration procedures introduced in this research. Section 4 discusses the advantages and disadvantages of this calibration method, and Sec. 5 concludes the work.

2 Principle

2.1 *DMD Image Generation*

In this research, we use a phase-shifting method to establish the correspondence between camera pixels and projector pixels. The same method is used in the structured light system for 3-D shape measurement. A calibration plane

0091-3286/2008/$25.00 © 2008 SPIE

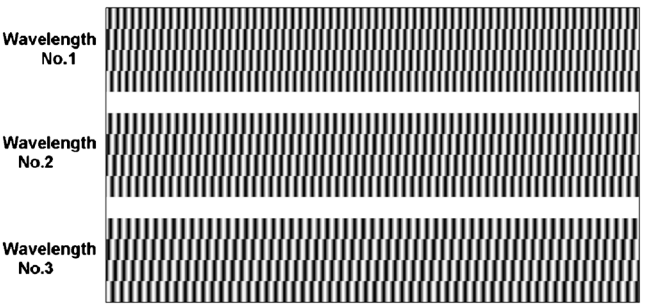

Fig. 1 Fringe patterns used in the structured light system.

with 99 (9×11) circles is positioned in the 3-D measurement volume. Then we project a series of sinusoidal phase-shifted fringe patterns (three synthetic wavelengths, each one with four phase shifts; see Fig. 1) onto the calibration plane and capture them. The captured images consist of a calibration plane image and some sinusoidal phase-shifted fringe patterns.

The sinusoidal phase-shifted fringe patterns are used to establish a one-to-one mapping between a CCD image and a DMD image. Based on a four-step phase-shifting algorithm, the actual phase at each pixel can be calculated, which is between 0 and 2π. If a multiple fringe pattern is used, a continuous unwrapped absolute phase map can be obtained by phase unwrapping.[15] We use the multifrequency heterodyne principle to obtain the unwrapped absolute phase value.[16,17] Then the unwrapped absolute phase map can be used to establish a one-to-one mapping between a CCD image and a DMD image.

After the absolute phase map is obtained, a unique point-to-line mapping between the CCD pixels and DMD pixels can be established. If vertical fringe patterns are used, this line is a vertical line. If horizontal fringe patterns are used, then this line is a horizontal line. If both vertical and horizontal fringe patterns are used, then the pixel at the intersection of these two lines is the pixel corresponding to the camera pixel on the DMD. Therefore, by using this method, we can establish a one-to-one mapping between a CCD image and a DMD image. The following paragraph explains the details of this method.

Figure 2 illustrates how the correspondence between the CCD pixels and the DMD pixels is established. We extract the subpixel position of each circle center from the calibration plane image, as shown in Fig. 2(a), using standard image-processing techniques.[18] Figure 2(b) and 2(c) are the absolute phase maps Φ_h,Φ_v in the horizontal and vertical directions. Let the coordinates of the upper left circle center p_1 be (x_1,y_1). Because (x_1,y_1) has subpixel accuracy, the absolute phases of the point p_1 in the two directions φ_h,φ_v can be obtained by linear interpolation. Then the coordinates of the corresponding point p_1', which has the same absolute phase in the two directions, can be calculated as follows:

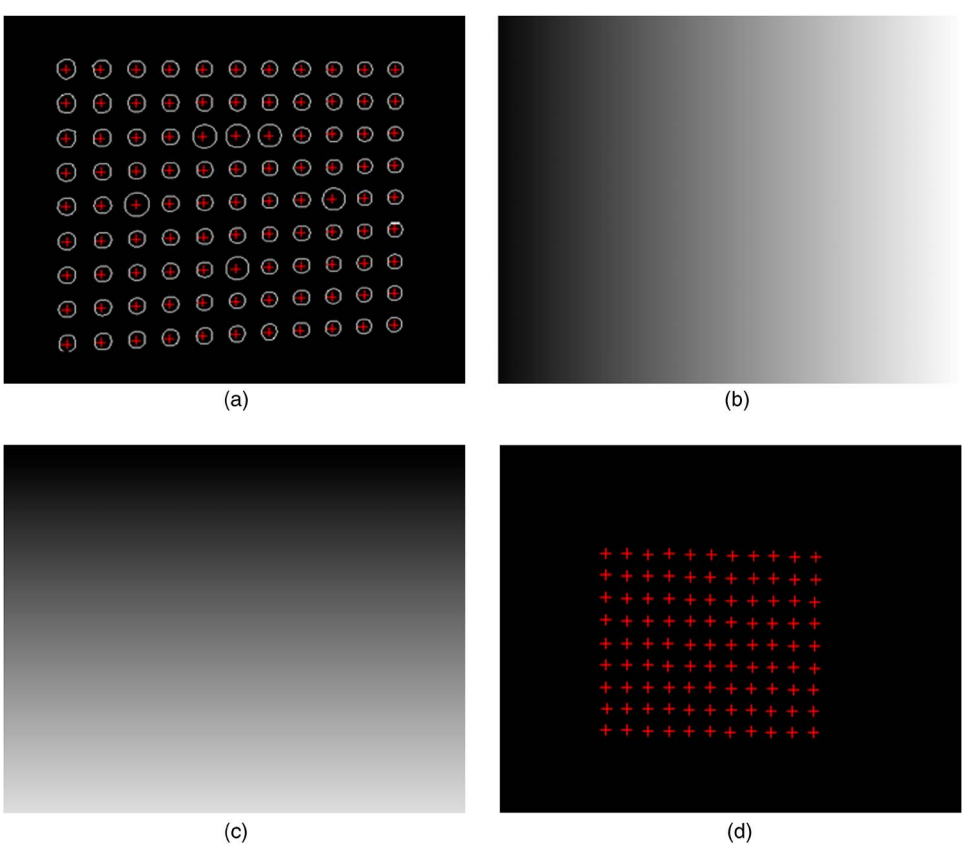

Fig. 2 CCD image and its corresponding DMD image: (a)CCD image, (b) horizontal absolute phase map, (c) vertical absolute phase map, (d) DMD image.

$$x = \frac{\varphi_v}{N_v \times 2\pi} \times W,$$
$$y = \frac{\varphi_h}{N_h \times 2\pi} \times H, \tag{1}$$

where N_v, N_h are the numbers of periods in the vertical and horizontal fringe patterns, respectively, and W and H are the width and height of the fringe patterns. The coordinates of the corresponding point p_1' are also of subpixel accuracy. According to this method, we can estimate all the corresponding points of the circle centers. Figure 2(d) shows the corresponding DMD image. One can verify the accuracy of the DMD image by projecting it onto the real calibration plane and checking its alignment. If the alignment is good, the DMD image created is accurate.

2.2 *Phase Error Compensation*

From the DMD image generation calculation flow, we can see that the precision of the actual phase will affect the precision of the corresponding point, and furthermore affect the precision of the system calibration. However, the nonlinear γ of the projector introduces some nonlinear phase error during the actual phase calculation process. The γ of any commercial projector is purposely distorted to be nonlinear to have better visual effect.[19] As a matter of fact, the inherent luminance nonlinearity of a display device can often be described with a simple pointwise operation of the form

$$w = u^{\gamma}, \tag{2}$$

where $u \in [0,1]$ denotes the normalized image pixel value, w is the normalized actual output intensity, and γ is a constant particular to the device. Typically a display device has a γ greater than 1.0, and the standard of the National Television System Committee recommends a γ of 2.2.[19] However, the actual γ of a digital video projector depends not only on its own factory preadjustment, but also on the computer system. In addition, some graphics cards dynamically vary the amount of γ correction for a balanced visual effect on the display.

We simulated the phase error caused by the nonlinear γ of the projector; the result is shown in Fig. 3. In this figure, we used 640 sampling points to show the concept. Figure 3(a) plots the input sinusoidal signal and output waveform (γ=2.2); Fig. 3(b) plots the real wrapped phase values and the ideal phase values for each sampling point. We subtract the ideal phase value from the real phase value for each point and obtain the phase error. The phase error caused by the nonlinear γ of the projector is plotted in Fig. 3(c).

In order to improve the accuracy of the correspondence, the effect of the nonlinear γ of the projector has to be eliminated during the projector calibration procedure. Recently, a lot of methods have been proposed to eliminate the phase error. Previously proposed methods, including the double three-step phase-shifting algorithm,[20] direct correction of the nonlinearity of the projector's γ,[21] and γ-correction technique based on statistical analysis of the fringe images,[19] demonstrated significant phase error reduction; however, the residual error remains nonnegligible.

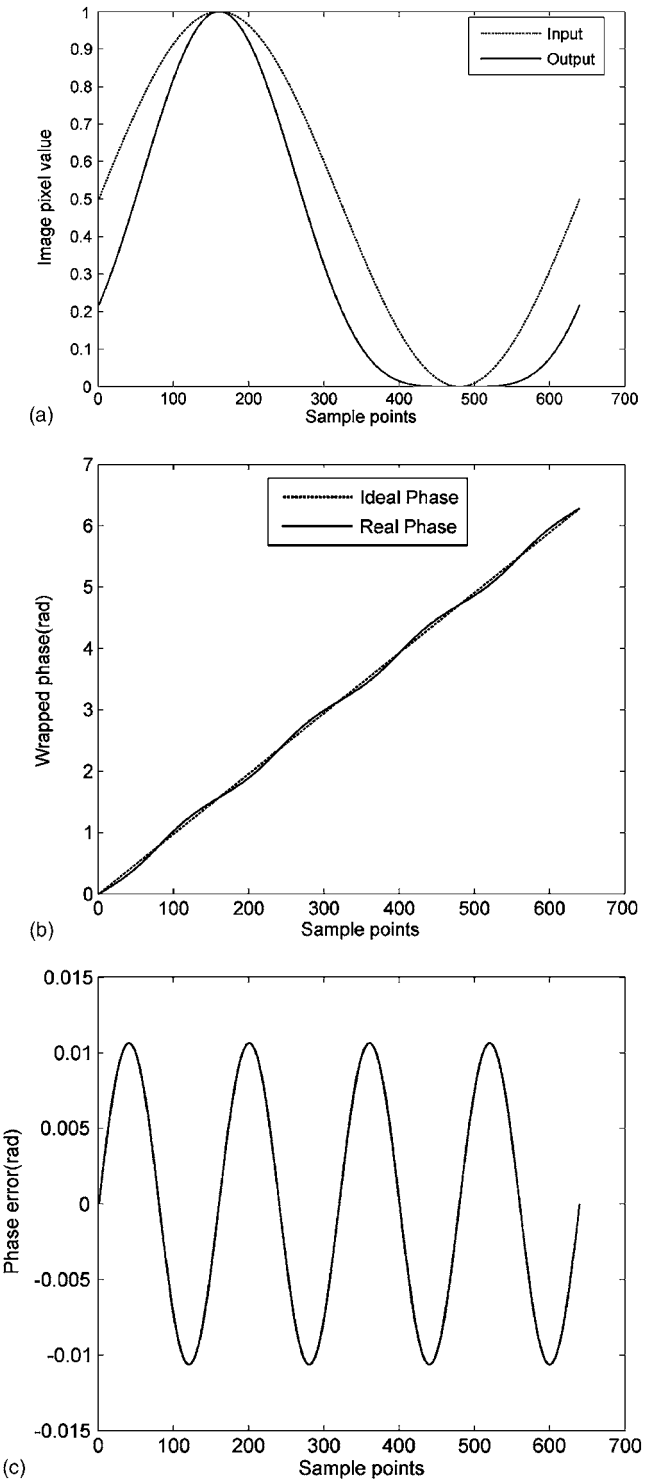

Fig. 3 Simulated result: (a) input sinusoidal signal and output waveform (γ=2.2), (b) real wrapped phase and ideal wrapped phase, (c) phase error caused by the nonlinear γ of the projector.

Zhang and Yau[22] proposed a method that does not require direct calibration of the γ of the projector and does not require γ to be monotonic. They captured a set of fringe images of a uniform flat surface board. The phase error of the captured fringe images is analyzed and stored in a LUT for phase error compensation. This method is simple and accurate.

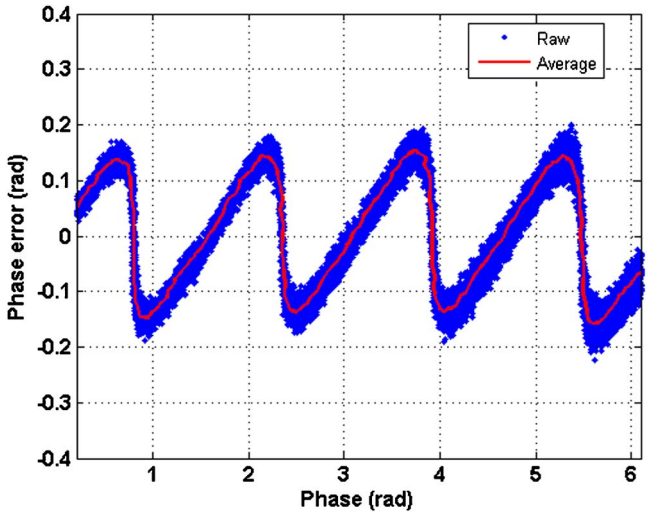

Fig. 4 Phase-error LUT.

So in this work, we create a 256-element error LUT according to Zhang and Yau's method.[22] We project four fringe images with the same phase shift as previously specified onto a uniform flat board, capture them, and compute the phase error. The phase errors for 50 row points are plotted in Fig. 4. We then divide the 2π period into 256 regions. For the k'th region, the phase value ranges from $(k-1)\times 2\pi/256$ to $k\times 2\pi/256$. The average error of the data points that belong to this region is stored in the k'th element of the LUT. The solid curve in Fig. 4 plots the errors stored in the LUT. The maximal phase error is 0.1538 rad.

Once the phase error LUT is created, it can be used for error compensation during projector calibration and 3-D measurement. For real captured fringe images, the phase computed from the fringe images can then be compensated by using this LUT. Assume the phase value for one point is φ_0, which belongs to region $k_0=[256\varphi_0/2\pi]$, where $[x]$ means the rounded-down integer value of x. Then the compensated phase is $\varphi=\varphi_0-\mathrm{LUT}(k_0)$.

According to the Sec. 2.1 and Sec. 2.2, we can get one data set, including the coordinates of the circle centers in CCD images and the coordinates of the corresponding points in a DMD image, for the system calibration. The data-set generation flow chart is shown in Fig. 5.

2.3 *System Calibration*

Once the input data are estimated, the next step is the estimation of the calibration parameters. Figure 6 shows the structured-light system used to test the proposed calibration procedure. In this system, the resolution of the charge-coupled device (DaHeng SV1410FM) is 1024×768 pixels with a nominal focal length of 25 mm, and the resolution of the DLP projector (Focus LP70) is 1024×768 pixels with a nominal focal length of 50 mm. The length of the base line is about 260 mm. The calibrated volume was about 800 mm wide, 600 mm tall, and 600 mm deep, placed 1300 mm from the system. A total of six images, as shown in Fig. 7, were captured by the camera from different positions. And the six corresponding DMD images created with the procedures described in Sec. 2.1 and Sec. 2.2 are shown in Fig. 8.

After a set of DMD images is generated, we can unify the calibration procedures of the structured light system and a classic stereo vision system. The MATLAB toolbox provided by Bouguet is used to calibrate the system.[23] We first calibrate the camera and the projector. The internal camera model is very similar to that used by Heikkila,[9] and the estimated intrinsic parameters are shown in Table 1. The parameters k_1,k_2 are the coefficients for the radial distortion; the parameters p_1,p_2 are the coefficients for the decentering distortion.

After the intrinsic parameters of the camera and the projector are calibrated, the next task is to calibrate the extrinsic parameters of the system. For this purpose, a unique world coordinate system for the camera and projector has to be established. In this research, a world coordinate system is established based on one calibration image set with its x and y axes on the plane, and its z axis perpendicular to the plane and pointing toward the system. Figure 9 shows the coordinate systems used in this work.

The purpose of extrinsic-parameter calibration is to find the relationships between the camera coordinate system and the world coordinate system, and also between the projector coordinate system and the same world coordinate system. These relationships can be expressed as

$$\mathbf{X}_c=\mathbf{M}_c\mathbf{X}_w,\qquad \mathbf{X}_p=\mathbf{M}_p\mathbf{X}_w, \tag{3}$$

where $\mathbf{X}_c=\{x_c,y_c,z_c\}^T$, $\mathbf{X}_p=\{x_p,y_p,z_p\}^T$, and $\mathbf{X}_w=\{x_w,y_w,z_w\}^T$ are the coordinate column vectors for point p in the camera, projector, and world coordinate systems, and $\mathbf{M}_c=[\mathbf{R}_c,\mathbf{t}_c]$ and $\mathbf{M}_p=[\mathbf{R}_p,\mathbf{t}_p]$ are the transformation matrices from the camera coordinate system and the projector coordinate system to the world coordinate system, respectively. Here $\mathbf{R}_c,\mathbf{t}_c$ and $\mathbf{R}_p,\mathbf{t}_p$ are matrices of the extrinsic parameters we should estimate. They can be obtained by the same procedures as those for the intrinsic parameters estimation. The only difference is that only one calibration image is needed to obtain the extrinsic parameters. The same MATLAB toolbox provided by Bouguet was is utilized to obtain the extrinsic parameters. Example extrinsic parameter matrices for the system setup are

$$\mathbf{M}_c=\begin{bmatrix} 0.9835 & 0.0663 & -0.1683 & -150.7701 \\ 0.0561 & -0.9963 & -0.0645 & 49.8310 \\ -0.1720 & 0.0540 & -0.9836 & 1308.1003 \end{bmatrix},$$

$$\mathbf{M}_p=\begin{bmatrix} 0.9139 & 0.0632 & -0.4010 & -112.8400 \\ 0.1030 & -0.9916 & 0.0784 & -159.2012 \\ -0.3927 & -0.1129 & -0.9127 & 1347.3015 \end{bmatrix}.$$

Once the system calibration is done, real measured object coordinates can be obtained based on the calibrated intrinsic and extrinsic parameters of the camera and the projector. The calculate method is similar to that described in the literature.[13]

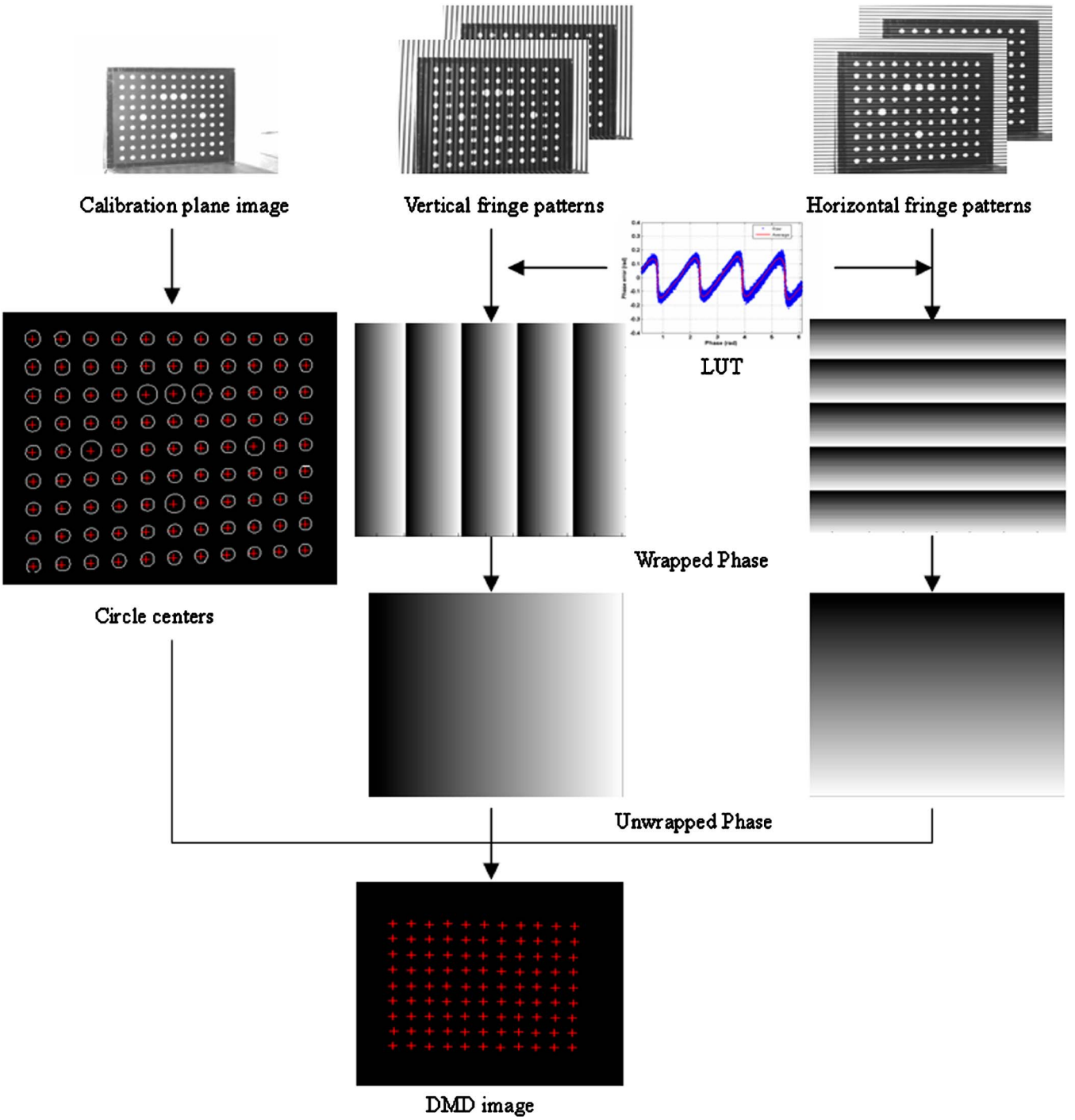

Fig. 5 Data-set generation flow chart.

3 Experiments and Calibration Evaluation

To evaluate the calibration method introduced in this research, we analyze the discrepancies obtained in the calibration. The reprojection error from the camera calibration is shown in Fig. 10, and the rms errors equal 0.09740 and 0.09039 pixels in the two directions. Similarly, the reprojection error in the projector calibration is shown in Fig. 11. The rms errors equal 0.14942 and 0.15707 pixels in the two directions.

To further verify the calibration accuracy, we measured a planar board with a white surface and reconstructed the 3-D coordinates using the estimated parameters. The measurement result is shown in Fig. 12(a). To determine the measurement error, we fit the measured coordinates with an ideal flat plane and calculate the distances between the measured points and the ideal plane. Figure 12(b) shows the measurement errors of all experimental numbers. The standard deviation is 0.043 mm (over a volume of 300

Fig. 6 The structured light system used to test the proposed calibration procedure.

$\times 200 \times 200$ mm^3). In addition, we measured a human face, and the result is shown in Fig. 13. The first image is a photograph of the face, and the second image is a 3-D model of it in shaded mode. The reconstructed 3-D model is very smooth, with details.

4 Discussion

As can be seen in the experimental results, the residual magnitude is small enough in both calibrations, as is expected of a good estimation.[8–12] One drawback of the estimations is the systematic distribution of the residuals, which indicate some error in the target position measurement. All the calibration procedures based on the knowledge of the 3-D coordinates of the target marks are affected by the uncertainty of the target measurement, and this is one of the most important sources of systematic error in calibration and reconstruction.[3] These errors can only be reduced by improving the accuracy of the target position or including a self-calibration strategy in the estimation.[6,8,24] However, this situation does not affect the present estimations too much, because the normalized stereo calibration error indicates that the residuals are negligible compared with image digitization noise at this depth.[25]

According to the LUT described in Sec. 2.2, the maximal phase error caused by the nonlinear γ of the projector is 0.1538 rad. The minimal number of periods in the sinusoidal phase-shifted fringe patterns used in this work is 59,[17] and the resolution of the fringe pattern is 1024×768 pixels. According to the formula (1), the maximal

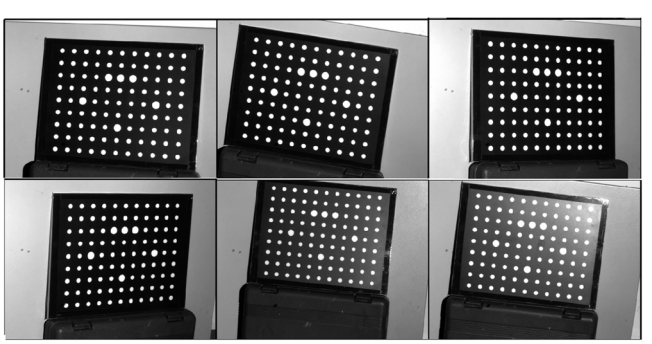

Fig. 7 Calibration plane images for camera calibration.

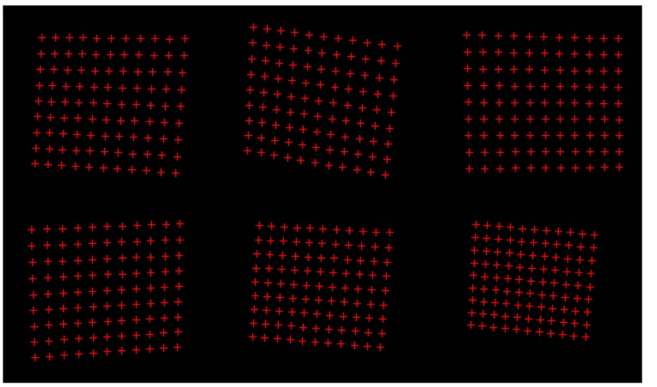

Fig. 8 Corresponding DMD images for projector calibration.

errors of the corresponding point in the DMD image caused by the nonlinear γ of the projector are equal to 0.4248 and 0.3186 pixels in the x and y directions, respectively. This result shows that the nonlinear γ of the projector indeed affects the accuracy of the correspondence between camera pixels and projector pixels. In order to further verify the effect of nonlinear γ of the projector on the precision of corresponding points in the DMD image, we obtained a group of corresponding points (P_1) without using the LUT to compensate the phase error during DMD image generation, and then computed the projections (P_2) in the DMD images of the circle centers based on the precalibrated intrinsic and extrinsic parameters of the projector. The errors between P_1 and P_2 are shown in Fig. 14. The rms errors equal 0.27963 and 0.24259 pixels in the two directions; they are much larger then the residuals obtained in the projector calibration. Therefore, it is necessary to eliminate the phase error caused by the nonlinear γ of the projector in the system calibration procedures. In this research, a small LUT was created and used to reduce the phase error in both

Table 1 Calibration results.

	Value	
Intrinsic parameter	Camera	Projector
α	3905.11823	2356.56238
β	3906.24932	2364.02100
γ	90 deg	90 deg
u_0	695.68818	515.34543
v_0	475.85129	821.95544
k_1	−0.01271	−0.08843
k_2	−3.45587	0.30651
p_1	−0.00180	−0.00464
p_2	−0.0296	0.03394

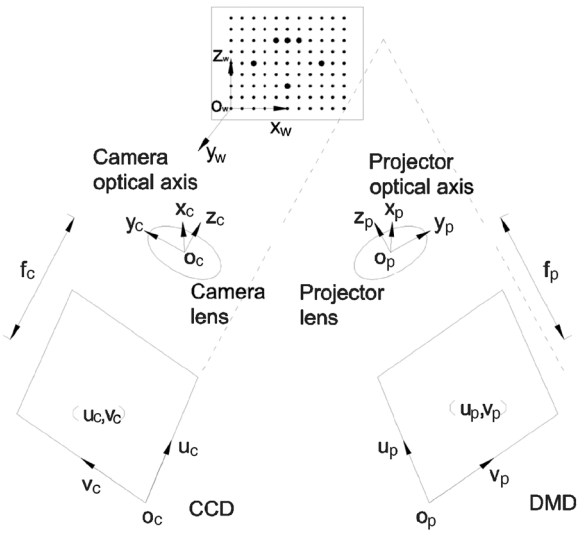

Fig. 9 The coordinate systems used in this work.

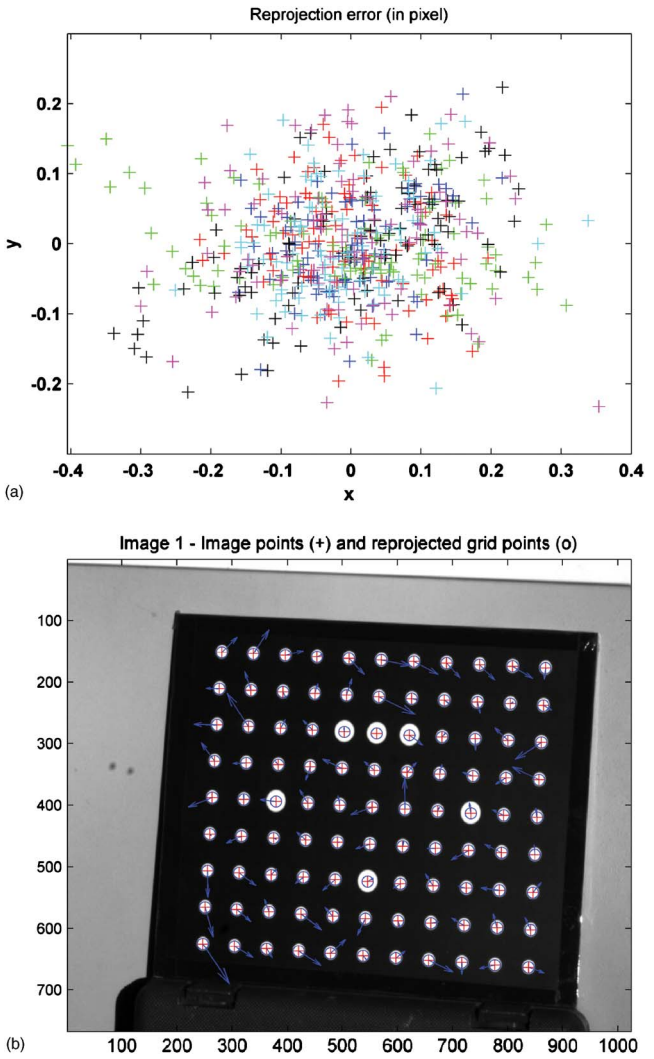

Fig. 10 Residuals obtained in the camera calibration: (a) reprojection error of the calibration images; (b) typical reprojection error distribution of one frame used in the calibration. In panel (b), + indicates the observed image position, ○ indicates the reprojected point, and the arrows indicate scaled residuals.

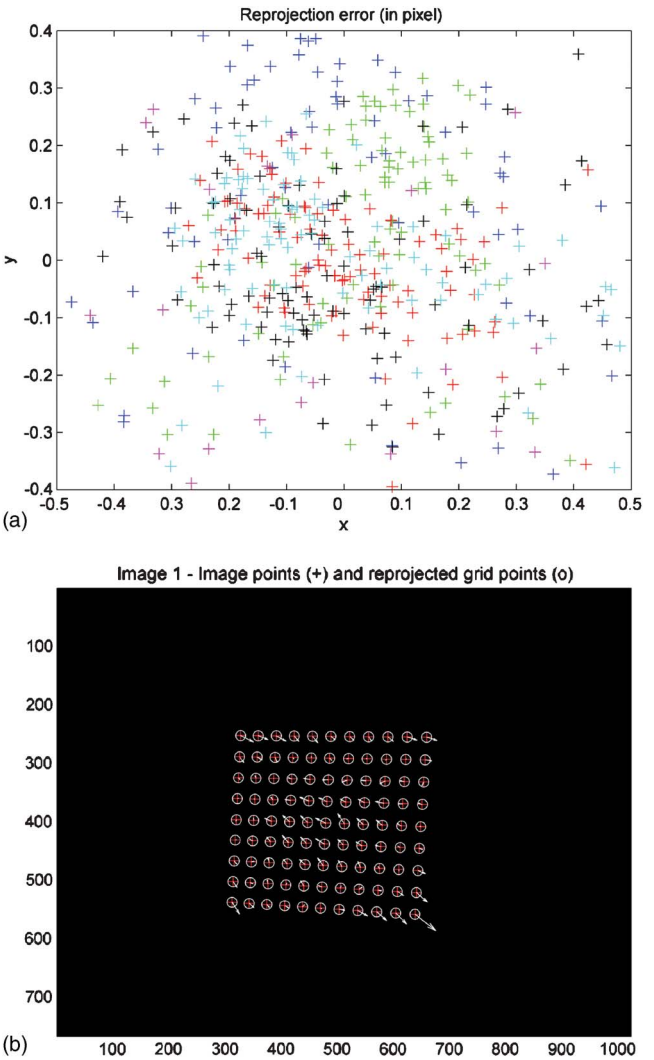

Fig. 11 Residuals obtained in the projector calibration: (a) reprojection error of the calibration images, (b) typical reprojection error distribution of one frame used in the calibration. In panel (b), + indicates the observed image position, ○ indicates the reprojected point, and the arrows indicate scaled residuals.

the calibration and the 3-D measurement. This method can significantly improve the accuracy of the correspondence and furthermore improve the accuracy of the projector calibration.

In addition, although 25 images were used to generate the DMD image, the process procedures, including circle center extraction, phase unwrapping, and corresponding point coordinate calculation, can be realized automatically through software within about 5 s. Furthermore, the calibration of the projector and that of the camera follow the same procedure. A calibration plane can be utilized to calibrate the camera and the projector simultaneously. So the system calibration method proposed in this work is easy and fast.

5 Conclusions

We present a novel accurate calibration method for the structured light system we developed. We treat the projector as a camera, and calibrate the camera and the projector

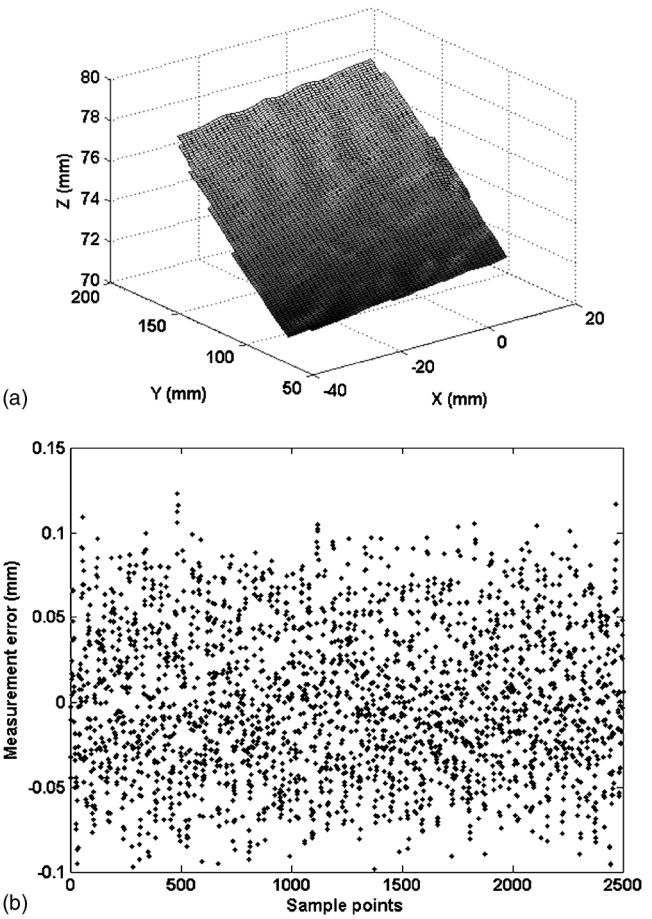

Fig. 12 3-D measurement result for the planar board: (a) 3-D plot of the measured plane, (b) measurement error of all experimental numbers.

independently using the traditional calibration method for cameras. Because the projector can be treated as a camera, the calibration of structured light systems becomes essentially the same as that of traditional stereovision systems, which is well established. A phase-shifting method is used to establish the correspondence between camera pixels and projector pixels. A precalibrated lookup table and a linear interpolation algorithm are proposed to improve the accuracy of the generated DMD image. After the corresponding DMD images were obtained, the MATLAB toolbox provided by Bouguet was used to calibrate the system. The

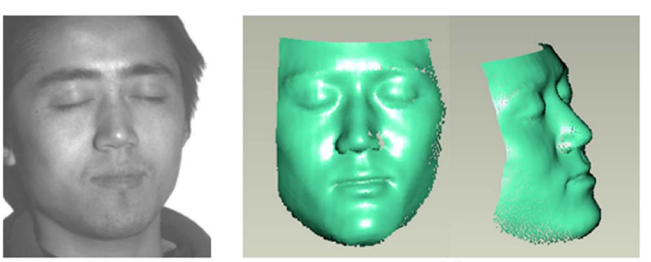

Fig. 13 3-D measurement result for a human face: (a) photograph, (b) 3-D model.

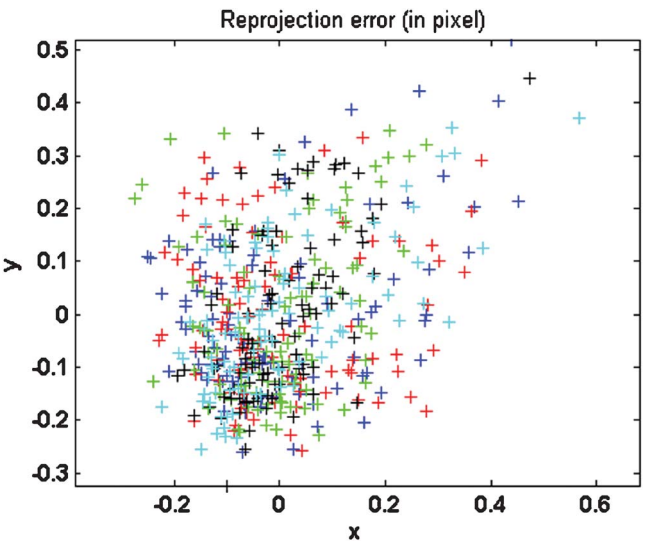

Fig. 14 The errors between P_1 and P_2.

experimental results show that the rms measurement error is 0.043 mm over a volume of $300 \times 200 \times 200$ mm^3 and the reconstructed 3-D model is very smooth and detailed.

Acknowledgment

This work was supported by the Eleventh Five-Year Preresearch Project of China.

References

1. F. Chen, G. W. Brown, and M. Song, "Overview of three-dimensional shape measurement using optical methods," *Opt. Eng.* **39**(1), 10–22 (2000).
2. S. Zhang and S.-T. Yau, "High-resolution, real-time 3D absolute coordinate measurement based on a phase-shifting method," *Opt. Express* **45**, 2644–2649 (2006).
3. R. Legarda-Sáenz, T. Bothe, and W. P. Jüptner, "Accurate procedure for the calibration of a structured light system," *Opt. Eng.* **43**(2), 464–471 (2004).
4. F. J. Cuevas, M. Servin, and R. Rodriguez-Vera, "Depth object recovery using radial basis functions," *Opt. Commun.* **163**(4), 270–277 (1999).
5. F. J. Cuevas, M. Servin, O. N. Stavroudis, and R. Rodriguez-Vera, "Multi-layer neural networks applied to phase and depth recovery from fringe patterns," *Opt. Commun.* **181**(4), 239–259 (2000).
6. C. C. Slama, *Manual of Photogrammetry*, American Society of Photogrammetry, Falls Church, VA (1980).
7. C. S. Fraser, "Photogrammetric camera component calibration: A review of analytical techniques," in *Calibration and Orientation of Cameras in Computer Vision*, A. Gruen and T. S. Huang, Eds., pp. 95–136, Springer-Verlag, Berlin (2001).
8. A. Gruen and H. A. Beyer, "System calibration through selfcalibration," in *Calibration and Orientation of Cameras in Computer Vision*, A. Gruen and T. S. Huang, Eds., pp. 163–194, Springer-Verlag, Berlin (2001).
9. J. Heikkila, "Geometric camera calibration using circular control points," *IEEE Trans. Pattern Anal. Mach. Intell.* **22**(10), 1066–1077 (2000).
10. F. Pedersini, A. Sarti, and S. Tubaro, "Accurate and simple geometric calibration of multi-camera systems," *Signal Process.* **77**(3), 309–334 (1999).
11. D. B. Gennery, "Least-square camera calibration including lens distortion and automatic editing of calibration points," in *Calibration and Orientation of Cameras in Computer Vision*, A. Gruen and T. S. Huang, Eds., pp. 123–136, Springer-Verlag, Berlin (2001).
12. Q. Hu, P. S. Huang, Q. Fu, and F. P. Chiang, "Calibration of a 3-D shape measurement system," *Opt. Eng.* **42**(2), 487–493 (2003).
13. S. Zhang and P. S. Huang, "Novel method for structured light system calibration," *Opt. Eng.* **45**(8), 83601–83608 (2006).
14. K. Hibino, B. F. Oreb, D. I. Farrant, and K. G. Larkin, "Phase shifting for nonsinusoidal waveforms with phase-shift errors," *J. Opt. Soc. Am. A* **12**, 761–768 (1995).

15. D. C. Ghiglia and M. D. Pritt, *Two-Dimensional Phase Unwrapping: Theory, Algorithms, and Software*, John Wiley and Sons, New York (1998).
16. C. Reich, R. Ritter, and J. Thesing, "3-D shape measurement of complex objects by combining photogrammetry and fringe projection," *Opt. Eng.* **39**(1), 224–231 (2000).
17. Z. W. Li, Y. S. Shi, C. J. Wang, G. Zhou, and D. Qin, "A prototype system for high precision 3D measurement based on grating method," *Proc. SPIE* **6834**, 683442 (2007).
18. C. Gonzalez and E. Woods, *Digital Image Processing*, 2nd ed., Publishing House of Electronics Industry, Beijing (2002).
19. H. Guo, H. He, and M. Chen, "Gamma correction for digital fringe projection profilometry," *Appl. Opt.* **43**(14), 2906–2914 (2004).
20. P. S. Huang, Q. Hu, and F.-P. Chiang, "Double three-step phase-shifting algorithm," *Appl. Opt.* **41**, 4503–4509 (2002).
21. P. S. Huang, C. Zhang, and F.-P. Chiang, "High-speed 3-D shape measurement based on digital fringe projection," *Opt. Eng.* **42**, 163–168 (2003).
22. S. Zhang and S.-T. Yau, "Generic nonsinusoidal phase error correction for 3-D shape measurement using a digital video projector," *Appl. Opt.* **46**(1), 36–43 (2007).
23. J. Y. Bouguet,"Camera calibration toolbox for Matlab," http://www.vision.caltech.edu/bouguetj/calib-doc.
24. W. Schreiber and G. Notni, "Theory and arrangements of selfcalibrating whole-body three-dimensional measurement systems using fringe projection technique," *Opt. Eng.* **39**(1), 159–169 (2000).
25. J. Salvi, X. Armangué, and J. Batlle, "A comparative review of camera calibrating methods with accuracy evaluation," *Pattern Recogn.* **35**(7), 1617–1635 (2002).

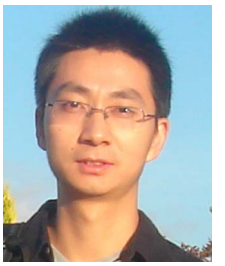

Zhongwei Li is a PhD student at Huazhong University of Science and Technology (HUST), China. He obtained his BS and MS degrees from the Department of Materials Science and Engineering of HUST in 2003 and 2006, respectively. His research interests include optical metrology, 3-D machine and computer vision image processing, and reverse engineering.

Yusheng Shi obtained his BS and MS degrees in mine exploration engineering from Wuhan Geology College, China, in 1984 and 1989, and his PhD degree in exploration and architecture engineering from China University of Geology in 1996. Since 1998, he has been a member of the Department of Materials Science and Engineering of the Huazhong University of Science and Technology, China, where he is currently a full professor. His research interests are mainly in the areas of advanced manufacturing technology, rapid prototyping, and laser processing.

Biographies and photographs of other authors not available.